Available online at www.sciencedirect.com
SCIENCE DIRECT
Applied Catalysis B: Environmental 59 (2005) 45–56
APPLIED CATALYSIS B: ENVIRONMENTAL
www.elsevier.com/locate/apcatb

Water-gas shift: an examination of Pt promoted MgO and tetragonal and monoclinic ZrO_2 by in situ drifts

Emilie Chenu, Gary Jacobs, Adam C. Crawford, Robert A. Keogh, Patricia M. Patterson, Dennis E. Sparks, Burtron H. Davis *

University of Kentucky, Center for Applied Energy Research, 2540 Research Park Drive, Lexington, KY 40511, USA

Received 30 August 2004; received in revised form 29 November 2004; accepted 17 December 2004
Available online 5 February 2005

Abstract

In situ DRIFTS measurements on unpromoted and Pt promoted MgO and ZrO_2 (both tetragonal and monoclinic) indicate that at high H_2O/CO ratios, where the reaction rate has been reported to be zero order in H_2O and first order in CO, the mechanism involved in the catalysis of water-gas shift is likely a surface formate mechanism, in agreement with Shido and Iwasawa. Pt was found to catalyze the removal of surface carbonates and to facilitate the generation of active OH groups relative to the unpromoted catalyst. Comparison with Pt/ceria revealed that the OH groups involved in the catalysis of magnesia and zirconia may be those of the bridging variety which occur at defect sites. That is, water dissociated over vacancies to produce bridging OH groups, as observed by infrared spectroscopy. The existence of such an adsorbed species is implied in the zero reaction order for water, where kinetics suggests that the surface should be saturated by an adsorbed water species. The lower extent of vacancy formation for magnesia and zirconia-based materials in comparison with ceria could explain a lower surface population of active bridging OH groups. CO was used as a probe molecule of the reduced centers, as it reacts with bridging OH groups to generate surface formates, a proposed WGS intermediate, and the decomposition of which is proposed to be the rate-limiting step. The trends in formate intensity by CO adsorption and CO conversion in WGS catalytic testing both followed the order: Pt/ceria > Pt/m-zirconia > Pt/t-zirconia > Pt/magnesia. In all cases, a normal kinetic isotope effect was observed in switching from H_2O to D_2O, consistent with a link between the rate-limiting step and the decomposition of surface formates, as noted previously by Shido and Iwasawa for Rh/ceria, MgO, and ZnO.

Keywords: Magnesia; MgO; Zirconia; ZrO_2; Tetragonal; Monoclinic; Platinum; Pt; Ceria; CeO_2; Vacancies; Water-gas shift; LTS; Kinetic isotope effect; KIE; DRIFTS

1. Introduction

The water-gas shift (WGS) reaction is receiving renewed interest for the production of H_2 from the steam reforming and partial oxidation of hydrocarbons [1–5]. One possible arrangement is that both high temperature (HTS) and low temperature shift (LTS) catalysts could be utilized in a stage-wise reactor after the steam reformer to convert CO, a poison for fuel cell electrodes, and in the process, generate more H_2.

Many recent studies focus on precious metal loaded ceria catalysts as highly active candidates for LTS, although deactivation phenomena still must be defined. Much of our recent research has focused on defining the active sites responsible for the catalytic activity of this catalyst system [6–8]. There is an important debate regarding whether metal/ceria catalysts operate via a support mediated redox process [9–13] (below, left), where one step is the reoxidation of reduced ceria by H_2O, or a reactant-promoted surface formate mechanism,

* Corresponding author. Tel.: +1 859 257 0253; fax: +1 859 257 0302.
E-mail address: davis@caer.uky.edu (B.H. Davis).

0926-3373/$ – see front matter © 2005 Elsevier B.V. All rights reserved.
doi:10.1016/j.apcatb.2004.12.013

one possibility of which is shown below on the right [14,15]:

$Pt + CO \rightarrow Pt\text{-}CO$

$Pt\text{-}CO + 2CeO_2 \rightarrow Ce_2O_3 + CO_2$

$H_2O + Ce_2O_3 \rightarrow 2CeO_2 + H_2$

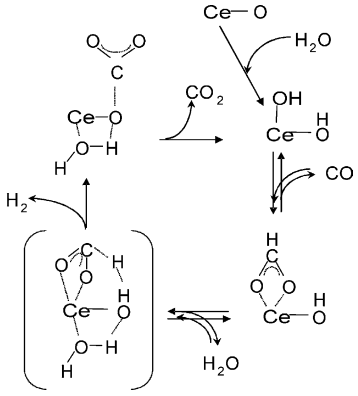

While the mechanism on the left has its history rooted in the oxygen-storage capacity of ceria, as applied in automobile catalytic convertor catalysis [9–13], the one on the right has developed from research on catalytic decomposition of formic acid [14–22]. The ceria-mediated redox mechanism accounts for the importance of oxygen vacancies to the active site, as it is implied that adsorbed CO on Pt reacts with ceria at the interface to generate CO_2, accompanied by a change in the oxidation state of Ce atoms involved with the vacancy from Ce^{4+} to Ce^{3+}. H_2O was suggested to reoxidize ceria to Ce^{4+}, with the liberation of hydrogen. A formate mechanism for WGS, on the other hand, is strongly supported by infrared spectroscopy investigations and the consideration of a normal kinetic isotope effect associated with formate decomposition. The importance of vacancies, as pointed out by proponents of the redox mechanism, is also emphasized to be a vital step in the generation of the active sites for the formate mechanism, which are bridging OH groups.

The decomposition of formic acid on oxides takes place at temperatures above 200 °C and proceeds in one of two directions or with mixed selectivity, depending on the choice of catalyst.

1. dehydration $HCOOH \Rightarrow CO + H_2O$
2. dehydrogenation $HCOOH \Rightarrow CO_2 + H_2$

In relation to catalytic WGS, it is the dehydrogenation pathway that is of particular interest for establishing the link with formic acid decomposition. In terms of selectivity, Mars [16] demonstrated that while some catalysts promoted the dehydration pathway (e.g., TiO_2, SiO_2, and Al_2O_3), others catalyzed dehydrogenation (e.g., MgO, ZnO, Fe_3O_4, ThO_2 after high temperature heating, and Cr_2O_3). It is clear that the catalysts employed for dehydrogenation of formic acid are precisely the same catalysts effective for carrying out catalytic WGS.

By closely correlating kinetic data with observations from in situ infrared spectroscopy, the conclusion was drawn [17] that an intermediate is involved in the decomposition of formic acid, and the stability governs the relative rates of dehydrogenation (route B) and dehydration (route C). The behavior of adsorbed formate ion, as observed in infrared spectroscopy and correlated to reaction testing results, led the researchers to conclude that it was the most likely intermediate for the reaction, and arises from the dissociative adsorption of formic acid [17]:

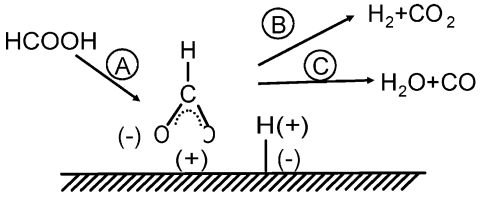

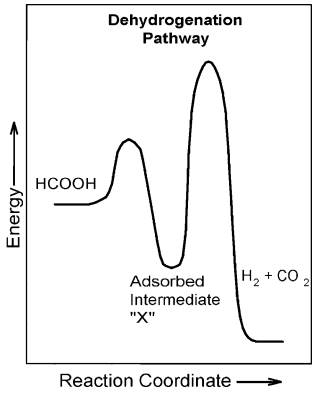

In such cases where the stability of the formate was found to be high, of particular interest to catalyst researchers studying the related water-gas shift reaction, the dehydrogenation coordinate put forth by Mars et al. [17] was schematically represented according to the above reaction pathway.

Since that time, and especially during the 1980s and early 1990s, many in situ infrared spectroscopy investigations and kinetic isotope effect studies were conducted aimed at exploring the adsorbed formate as an important intermediate for water-gas shift. Some notable studies include a series of publications by Iwasawa and coworkers [14,15,23–25], who studied water-gas shift over ZnO, MgO, ceria, and Rh promoted ceria.

Considering the trend in catalysis regarding the use of metal/oxide catalysts in fuel processors for PEM fuel cell applications, reviewing this historical perspective is important. In the case of water-gas shift, CO has been shown to react with active surface hydroxyl groups to produce surface formates. In the case of a partially reducible oxide (e.g., ceria, thoria, etc.), there is increasing evidence to

support the view that surface shell reduction leads to surface hydroxyl groups which are claimed to be active sites for water-gas shift. The first study to show the generation of surface formates on the surface of partially reduced ceria may have been that of Onishi's group [26]. However, formates have been observed by many other groups since that time [6–8,14,15]. In a recent study [27], we compared the formate bands arising from the adsorption of HCOOH and DCOOH with those arising from the adsorption of CO to bridging OH and OD groups and have found that they coincide precisely. It is important to note that the active bridging OH group densities depend on the degree of reduction of the surface shell of ceria. Much more intense formate bands are observed upon CO addition to Rh or Pt/ceria at 250 °C than on unpromoted ceria, due to the ability of the noble metal to facilitate the surface reduction process [7,8,14]. Differences between OH groups on fully oxidized and partially reduced ceria are reported.

For partially reduced ceria, bands for OH groups have been observed at considerably lower wavenumbers than those of the terminal groups (i.e., Type I) for the oxidized form of ceria (i.e., Ce^{4+} oxidation state). For example, for unreduced ceria, the Type I groups appear at between 3690 and 3710 cm^{-1} [28–30]. However, after a reduction in hydrogen of unpromoted ceria (occurring at ca. 450 °C), or at much lower temperatures with Pt or Rh addition (e.g., 200–250 °C), sharp bands are formed in the infrared spectrum at approximately 3650 cm^{-1} [7,8,14], assigned to Type II bridging OH groups on partially reduced ceria.

If one considers the WGS reaction from the redox perspective, vacancies are considered to be involved in the reaction mechanism. The reaction is catalyzed by the presence of a metal, and it is well established that the metal promotes the surface reduction of the oxide. Some direct evidence includes our recent work using XANES spectroscopy [8], a method that had already been applied to ceria-based catalysts in the past [31,32]. However, in exploring the possibility of a redox mechanism, evidence to show that H_2O rapidly reoxidized the partially reduced ceria at low temperature in a hydrogen-containing environment was not obtained [8]. Rather, by infrared spectroscopy, we observed that on partially reduced ceria, OH bands were present with considerably lower wavenumbers than those identified on fully oxidized ceria, in agreement with others [14,15,22,28–30].

Therefore, it was concluded that the Type II bridging OH groups were associated with reduced centers on the ceria surface. In considering the redox perspective, and the importance of vacancies to the reaction, the bridging OH groups could be interpreted to be the interaction of a vacancy with water—i.e., via dissociation of water. If one considers that a vacancy is the removal of O (i.e., a reduction process resulting in the lowering of two Ce atoms to the Ce^{3+} oxidation state), then the dissociation of water under net reducing conditions will not change the oxidation state further. Rather, one would expect the appearance of two OH groups on the surface corresponding to two reduced Ce centers, or from the perspective of the redox mechanism, corresponding to one vacancy.

The bridging OH group formation under H_2 treatment is promoted to low temperatures (e.g., 200–250 °C range) when noble metals like Rh or Pt are present [6–8,14]. One possibility for the promoting effect is that bridging OH group formation may circumvent vacancy formation, with Pt allowing the dissociation and spillover of H-atoms to the surface of ceria, such that the bridging OH groups are formed directly. Again, for every two H-atoms on the surface, there must be a change in the oxidation state of two Ce atoms from Ce^{4+} to Ce^{3+}, as shown in the schematic. Both routes of bridging OH group formation are shown below for ceria:

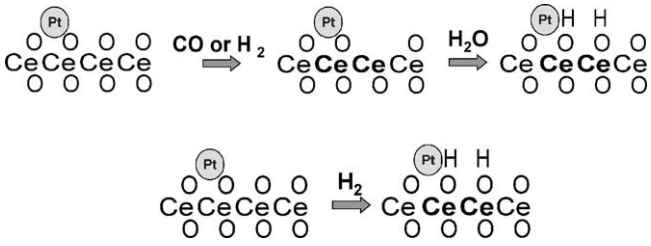

The reduced defect centers, with Ce^{3+}, are displayed in bold type.

Such bridging OH groups have also been observed on thoria [33,34] and zirconia [35,36]. The link between the generation of the bridging OH groups and the partial reduction of ceria was established by comparing the IR band intensities at different temperatures to the surface shell reduction process as measured by temperature programmed reduction [6,7], and more directly, by in situ XANES [8].

The present study concerns the nature of the active site during low temperature WGS under conditions relevant to a fuel cell processor. In these studies, we are operating at a high H_2O/CO feed ratio, typical of conditions after secondary water injection and following that of the first high temperature shift stage of a fuel processor. Even so, we have not added CO_2 to the feed stream, although CO_2 must be considered from the standpoint of engineering [37].

The kinetics of the WGS reaction over metal/ceria catalysts, when a high CO/H_2O ratio is employed, shows a zero order dependency on the partial pressure of CO [10,12], while at high H_2O/CO ratios, the conditions in which we are working at, the order of the partial pressure of water is close to zero while the order of the partial pressure of CO is close to unity [12]. For a zero order dependency on H_2O, it is implied that the catalyst surface is close to saturation by an adsorbed H_2O species. Certainly, under those conditions, bridging OH groups are a strong possibility.

In either mechanism, the role of noble metal—for example, Pt—has been demonstrated to facilitate the surface reduction of ceria, which does involve changes in infrared band intensity and position [29,34] as well as removal of

surface carbonates [6–8]. It was of interest, in reexamining the oxides shown to be active for dehydrogenation of formic acid, to explore MgO promoted with Pt. Regarding zirconia, both monoclinic and tetragonal phases were selected on the basis that bridging OH groups have been observed on the surface by in situ DRIFTS experiments involving reactions of alcohols, and because Pt/ZrO_2 has been proposed to undergo partial reduction [38] via vacancy formation, an important step in the heterogeneously catalyzed CO_2 reforming of methane reaction [39] and the $t \rightarrow m$ phase transition [40,41]. The goal of the current investigation was to determine if the bridging OH groups associated with defect centers (i.e., vacancies) could be formed on the surfaces of these materials, utilize CO as a probe molecule of the bridging OH groups based on the formate intensity, obtain a ranking by testing in the fixed bed reactor, and finally, conduct isotope switching in the reactor to assess for a kinetic isotope effect consistent with a formate mechanism for the high H_2O/CO condition.

2. Experimental

2.1. Catalyst preparation

2.1.1. Magnesia

High surface area magnesia was prepared by homogeneous precipitation of magnesium nitrate first with urea as the precipitating agent, followed by aqueous ammonia. The method, explained in some detail in [42], was employed by Flytzani-Stephanopoulos and coworkers [12,13] for preparing high surface area ceria LTS catalysts. Urea decomposition is a slow process providing a slower, more homogeneous precipitation, resulting in oxide materials with higher surface areas than standard precipitation methods. Appropriate amounts of $Mg(NO_3)_2$ and urea (Alfa Aesar, 99.5%) were dissolved in deionized water, and to the solution NH_4OH (Alfa Aesar, 28–30% NH_3) was added dropwise (∼1 ml/min). The mixture was boiled at 100 °C with constant stirring. The precipitate was filtered, washed with 600 ml of boiling deionized water, and dried in an oven (100 °C) overnight. The dried precipitate was then crushed and calcined in a muffle furnace at 400 °C for 4 h.

2.1.2. Tetragonal phase zirconia

High surface area tetragonal zirconia was also prepared via homogeneous precipitation of the nitrate with urea as the precipitating agent. An appropriate amount of zirconyl nitrate hydrate and urea (Alfa Aesar, 99.5%) were dissolved in 900 ml of deionized water, and to the solution about 30 ml NH_4OH (Alfa Aesar, 28–30% NH_3) was added dropwise (∼1 ml/min). The mixture was then boiled at 100 °C with constant stirring. The precipitate was filtered, washed with 600 ml of boiling deionized water, and dried in an oven (100 °C) overnight. The dried precipitate was then crushed and calcined in a muffle furnace at 400 °C for 4 h.

2.1.3. Monoclinic phase zirconia

The monoclinic zirconia catalyst was prepared using a reflux method similar to that described by Clearfield [43]. A mixture of 300 ml of 0.6 M $ZrCl_4$ and 300 ml of 0.3 M NH_4OH was gently refluxed for 65.25 h. The solution at the end of the reflux period became milky in appearance. After the solution was cooled to room temperature, the pH was slowly adjusted from 1 to 10 with concentrated NH_4OH (15.8 M). The final precipitate was filtered and washed until a negative chloride test was obtained. The precipitate was dried overnight at 110 °C. The dried material was calcined in air at 500 °C for 4 h.

2.1.4. Pt addition

Incipient wetness impregnation (IWI) was employed to load Pt to 1% for each catalyst oxide and tetraamine platinum (II) nitrate was the salt. After loading, the catalyst was dried at 110 °C and then calcined at 400 °C for 4 h in a muffle furnace.

2.1.5. BET surface area

BET surface area measurements were carried out in a Micromeritics Tristar 3000 gas adsorption analyzer. In each trial, a weight of approximately 0.25 g of sample was used. The adsorptive gas was nitrogen (N_2) and the adsorption was carried out at the boiling temperature of liquid nitrogen.

2.1.6. Temperature programmed reduction

TPR was conducted on unpromoted and Pt promoted oxide catalysts using a Zeton-Altamira AMI-200 unit, which was equipped with a thermal conductivity detector (TCD). Argon was used as the reference gas, and 10% H_2 (balance Ar) was flowed at 30 cm^3/min as the temperature was increased from 50 to 800 °C at a ramp rate of 10 °C/min.

2.1.7. Diffuse reflectance infrared Fourier transform spectroscopy (DRIFTS)

A Nicolet Nexus 870 was used, equipped with a DTGS-TEC detector. A high pressure/high temperature chamber fitted with ZnSe windows was utilized as the WGS reactor for in situ reaction measurements. The gas lines leading to and from the reactor were heat traced, insulated with ceramic fiber tape, and further covered with general purpose insulating wrap. Scans were taken at a resolution of 4 to give a data spacing of 1.928 cm^{-1}. Typically, 128 scans were taken to improve the signal to noise ratio. The sample amount utilized was 33 mg of catalyst.

A steam generator consisted of a downflow tube packed with quartz beads and quartz wool heated by a ceramic oven and equipped with an internal thermocouple. The lines after the steam addition were heat traced. The steam generator and lines were run at the same temperature as that at the in situ sample holder of the DRIFTS cell. This allowed us to accurately bring the reactants to the desired reaction temperature. Water was added to the steam generator by

a thin needle welded to a 1/16 in. line. A precision ISCO Model 500D syringe pump was used to feed the water.

Feed gases were controlled by using Brooks 5850 series E mass flow controllers. Iron carbonyl traps consisting of lead oxide on alumina (Calsicat) were placed on the CO gas line. All gas lines were filtered with Supelco O_2/moisture traps.

2.1.8. X-ray absorption near edge spectroscopy (XANES)

XANES spectra at the Zr K-edge (17997.6 eV) were recorded at the National Synchrotron Light Source (NSLS) at Brookhaven National Laboratory (BNL) in Upton, New York at beamline X-18b. The X-rays were tuned by a Si(1 1 1) double crystal monochromator, which was detuned slightly to prevent glitches from harmonics. The catalyst was mixed 1:10 with boron nitride and gently pressed into a disk and loaded into an in situ XAS cell. The sample was treated with a mixture of hydrogen and helium (1:3) and analyzed at room temperature and 300 °C. The gases were mixed in a manifold and passed through an oxygen/water trap prior to entering the cell.

3. Results and discussion

3.1. XRD and TPR profiles

An XRD profile of the high surface area magnesia is reported in Fig. 1 (left). Integral breadth analysis of the peak situated at 2θ of 42.9° indicated that the domain size of the magnesia crystallites was close to 4.0 nm, consistent with a high surface area material. BET measurements indicated that the surface area was 185 m^2/g (pore volume: 0.368 cm^3/g). XRD profiles for the high surface area zirconia materials are displayed in Fig. 1 (right). As pointed out by Srinivasan et al. [44], it is difficult to assign cubic and tetragonal structures from XRD, since the peak positions are very close. However, the tetragonal structure can be differentiated from the cubic by the presence of characteristic splittings of the tetragonal phase, including (0 0 2) (2 0 0), (1 1 3) (3 1 1), (0 0 4) (4 0 0), and (0 0 6) (6 0 0). The cubic phase, on the other hand, only gives single peaks for each position. It is indicated in Fig. 1 (right) that the bottom profile is tetragonal by the observed (0 0 2) (2 0 0) splitting, while the monoclinic phase is easily identified at the top by the (1 1 1) (1 1 1) and (0 0 2) (0 2 0) (2 0 0) splittings. Line broadening analysis on the peaks corresponding to $(1\ 1\ 1)_m$ at 2θ of 28.2° and $(1\ 1\ 1)_t$ at 2θ of 30.4° was carried out to estimate the crystallite domain size for the two catalysts. The average zirconia crystallite diameter for the monoclinic sample was found to be approximately 8.6 nm, while the corresponding crystallite diameter for the tetragonal sample was slightly larger, at 10.7 nm. Results of BET surface area analysis indicated that the two materials had similar surface area, with the tetragonal phase catalyst being 93.3 m^2/g (pore volume: 0.074 cm^3/g) and the monoclinic being 91.3 m^2/g (pore volume: 0.174 cm^3/g). The high surface area preparations made the materials well-suited for adsorption experiments using infrared spectroscopy.

TPR profiles are reported in Fig. 2. Bulk ceria reduces above 700 °C, as shown in profile (a). As we have noted before [8], there is a broad peak between 400 and 500 °C which is associated with carbonate removal and surface shell reduction (profile (b)). Finally, Pt catalyzes the reduction this surface reduction process to lower temperature—ca. 250 °C, as indicated by profile (c), and recently confirmed by XANES experiments [8]. Comparing the unpromoted MgO material (profile (d)) to unpromoted ceria, there is a peak situated in 400–500 °C, suggesting that carbonates are removed at this temperature, and that surface oxygen atoms could be removed as well, leading to oxygen deficiencies at the surface. An amount of 1% Pt addition only shifted the major peak in the surface reduction process slightly to about

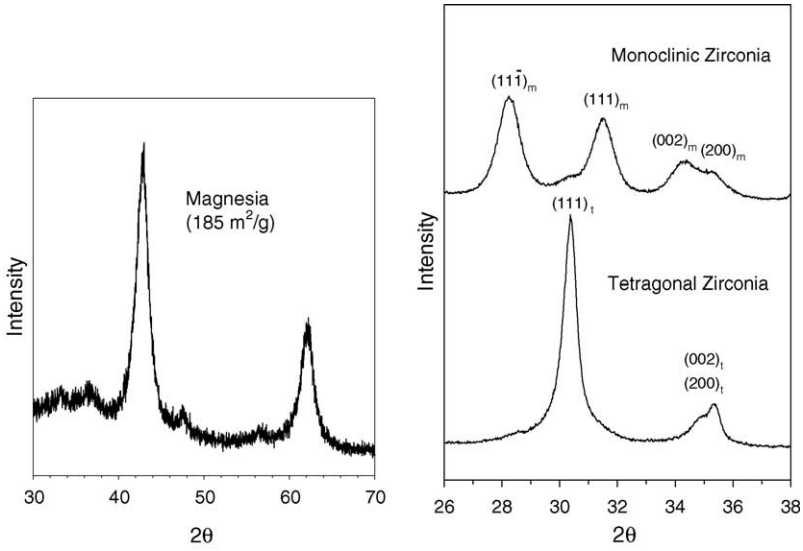

Fig. 1. XRD profiles for the (left) magnesia and (right) tetragonal and monoclinic zirconia samples.

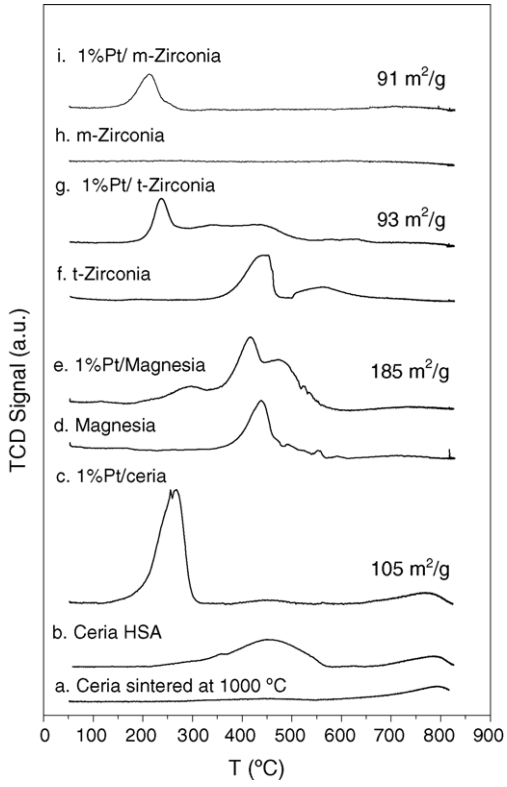

Fig. 2. Hydrogen TPR profiles for, moving upward, (a) ceria sintered at 1000 °C, (b) high surface area ceria, (c) 1% Pt/ceria, (d) magnesia, (e) 1% Pt/magnesia, (f) tetragonal zirconia, (g) 1% Pt/tetragonal zirconia, (h) monoclinic zirconia, and (i) 1% Pt/monoclinic zirconia.

390 °C, as indicated by profile (e). However, a low temperature shoulder was apparent at about 280 °C, as well as a high temperature shoulder at approximately 450 °C. Clearly, the overall area for all of the TPR peaks for hydrogen consumption was larger for the MgO sample with Pt—this suggests that Pt may enhance the surface reduction process, as observed in the case of ceria.

TPR measurements are also reported in Fig. 2 for unpromoted and Pt-promoted monoclinic and tetragonal zirconia samples. For the tetragonal catalyst (profile (f)), there is a pronounced peak at approximately 425 °C. This may indicate the liberation of water due to further crystallization, or could be due to the freeing of carbonate species. Interestingly, while carbonate species were also observed in infrared spectroscopy for the tetragonal phase, they were virtually absent for the monoclinic sample, which exhibited no peaks in TPR (profile (h)). Pt reduction and the formation of vacancies at the surface lead to the uptake of hydrogen at 200–250 °C for the tetragonal sample (profile (g)). This peak for the monoclinic sample is positioned at about 25 °C lower temperature than the tetragonal, as indicated by profile (i). The Pt apparently catalyzes the liberation of the surface carbonate as well, as broad peaks extend from 250 to about 450 °C.

For ceria, we suggested that Pt may promote removal of oxygen from the ceria surface, and that the vacancies could react with water to produce bridging OH groups. Or, another possibility is that the Pt could dissociate hydrogen to generate the bridging OH groups directly, again with a change in oxidation state for cerium atoms involved [8]. Both options may be possible for the Pt/magnesia and Pt/zirconia samples as well. However, judging by the rather small sizes of the peaks from the TPR profiles, the 1% Pt/ceria surface layer appears to be more easily reduced from the standpoint of kinetics. The extent of reduction in the low temperature range is also much higher for the Pt/ceria catalyst. Nevertheless, a limited surface reduction of Pt/magnesia and Pt/zirconia indicates the possibility that bridging OH groups could form on defect sites, albeit at lower concentrations than Pt/ceria.

3.2. *In situ DRIFTS of the reduction of MgO, Pt/MgO*

In situ DRIFTS spectra for the reduction of the Pt/magnesia and Pt/zirconia materials, shown in Fig. 3, are strikingly similar to the spectra we previously reported for Pt/ceria. That is, there are bands in the 1600–1250 cm^{-1} region that are typical of the OCO asymmetric and symmetric vibrations of surface carbonate species. With reduction in hydrogen, significant removal of carbonate bands occurred. However, for Pt/ceria, carbonate removal occurred up to 250 °C, the temperature at which the bridging OH groups were formed, clearly identified by absorption bands at 3650 cm^{-1}, with a shoulder at 3675 cm^{-1}. For unpromoted magnesia, the removal of carbonates is observed between 500 and 600 °C (Fig. 3A). With carbonate removal, OH group formation was clearly evident by the appearance of two bands at approximately 3730 and 3750 cm^{-1}. The presence of two bands suggests the possibility of bridging OH groups by dissociation of water on the vacancies formed (Fig. 3B). Addition of Pt facilitated carbonate removal at much lower temperatures, ca. 450 °C, as shown in Fig. 3A. The bridging OH groups were much more intense after reduction at 450 °C as compared to the unpromoted catalyst (Fig. 3B). There have been numerous studies [e.g., 45,46] indicating that vacancies can form on the surface of magnesia during a reduction treatment. The carbonate removal process, as observed by infrared spectroscopy, may provide information on the temperature at which this occurs. In a recent theoretical analysis [45] of the adsorption of water on MgO surfaces with defects such as F (when O atoms are removed from the surface), V (when Mg atoms are removed from the surface), and P (simultaneous removal of O and Mg atoms), the adsorption and dissociation properties of H_2O were found to strongly depend on the presence and absence of vacancies. The F-type vacancies, those suggested to be present in this work, were found, in general, to promote better conditions for the water coverage process, yielding more adsorbed water molecules and larger average binding energies [45].

Also, a recent theoretical study of formic acid decomposition via dehydrogenation indicated that the presence of

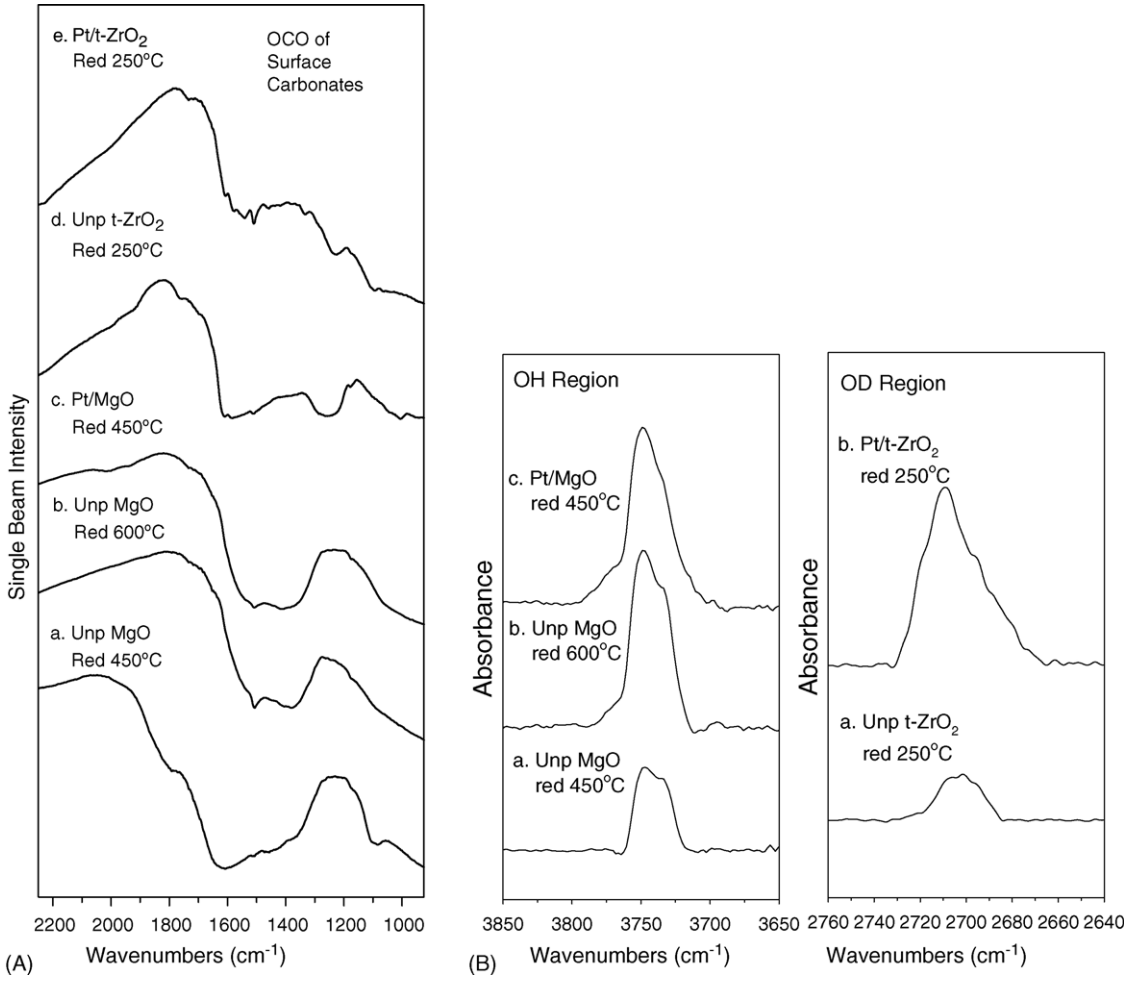

Fig. 3. (A) Comparison between residual OCO stretching bands of carbonates between unpromoted and Pt promoted MgO and t-ZrO_2 catalysts. Pt facilitates removal of surface carbonates (conditions: MgO-based catalysts, H_2:N_2 = 100 ccm:135 ccm; t-ZrO_2-based catalysts, D_2:N_2 = 100 ccm:135 ccm). (B) Comparison between intensity of bridging OH (or OD) groups on MgO and t-ZrO_2 catalysts, respectively, after reduction in H_2 (or D_2). Pt promotion facilitates the formation of bridging OH (or OD) groups in comparison with the unpromoted oxide.

defects are essential for the reaction to even be feasible over magnesia [46]. When defects are present, the reaction mechanism involves dissociative chemisorption of the formic acid to a formate species interacting with the vacancy. The transition state was found to involve C–H bond breaking, as discussed previously by Shido and Iwasawa [14,15] for the WGS reaction. The first adsorption step produces the first –OH group on the surface by dissociation of formic acid into formate (–OOCH) and (–H). The second step, involving C–H bond breaking, generates a second –OH group on the surface of MgO. Considering that these two –OH groups are possibly involved in the formic acid decomposition, and that the modeling study strongly indicates that defect sites are necessary for formic acid decomposition, we make the following suggestion for WGS. That is, bridging OH groups are likely important for the WGS reaction on Pt/MgO, especially under high H_2O/CO ratios, due to the high surface coverages by adsorption of H_2O.

For vacancy formation in magnesia, modeling calculations [45] have indicated that there is a general lowering of Mg charge associated with the F center formation when compared with the Mg charge associated with a defect-free MgO surface, and this is accompanied by an increase in the negative charge associated with the remaining oxygen atoms of the surface (i.e., enhanced basic character). As discussed previously, the bridging OH groups may be viewed as dissociated water over a vacancy.

3.3. In situ DRIFTS and XANES of the reduction of ZrO_2, Pt/ZrO_2

Similar conclusions apply for the ZrO_2 and Pt/ZrO_2 catalysts. The absorption bands present when the catalyst was initially charged into the DRIFTS were very similar to the carbonate bands previously observed on thoria and ceria-based catalysts [34], and for magnesia. In the case of unpromoted ZrO_2, as we previously observed with unpromoted ceria, the bands did not decompose in hydrogen until temperatures between 400 and 500 °C were obtained. Addition of Pt, as observed with ceria, allow significant

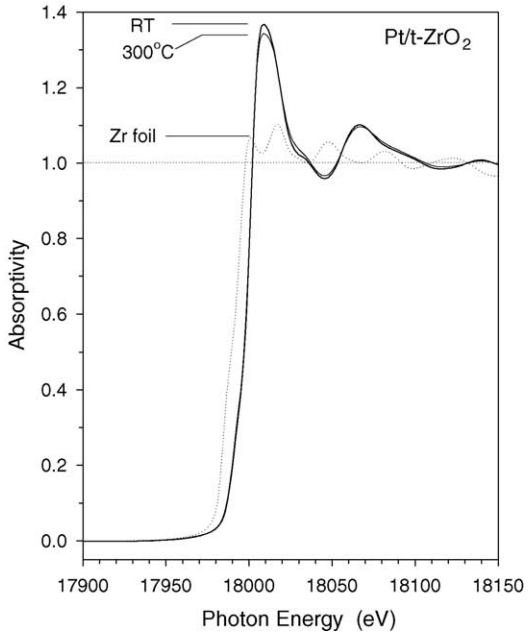

Fig. 4. Normalized XANES spectra for the reduction of 1% Pt/t-ZrO_2 in hydrogen/helium mixture (1:3). Zr foil shown as dotted line spectrum.

decomposition of the carbonate bands to be achieved by 250 °C (Fig. 3A). This was accompanied by bridging OH group formation, previously identified on zirconia catalysts [35,36], as shown in Fig. 3B.

Zirconia has been considered to be irreducible by many. However, the use of zirconia as an oxygen sensor in auto catalyst systems requires non-stoichiometric zirconia at higher temperatures. Non-stoichiometry in catalysis is consistent with the role of oxygen migration and vacancies in Pt/ZrO_2 catalysts helping to clean the metal surface during the dry reforming of methane reaction (i.e., CO_2 reforming of methane), used to produce syngas [39,47,48]. Fig. 4 shows spectra for fully oxidized ZrO_2, with its strong white line indicating a high density of available states above the Fermi level, and fully reduced Zr, for which the white line is absent. Treatment in hydrogen of Pt/ZrO_2 at 300 °C reveals a small, but measurable decrease in the white line intensity of Zr consistent with a surface reduction process (i.e., formation of vacancies or their associated bridging OH groups). The formation of zirconium atoms with oxidation state Zr^{3+} in the surface of the oxide has been reported during hydrogen treatment of zirconia in the 227–500 °C range [38], and, based on analogy with cerium, this process is suggested to be facilitated by the presence of Pt promoter.

3.4. In situ DRIFTS of the adsorption of CO and WGS reaction

Recently, we have demonstrated that formates are formed upon adsorption of CO to the bridging OH groups (i.e., associated with defect sites) of partially reduced ceria, and the intensity of formates gives an important indication of the number of active sites, and consequently, activity [7].

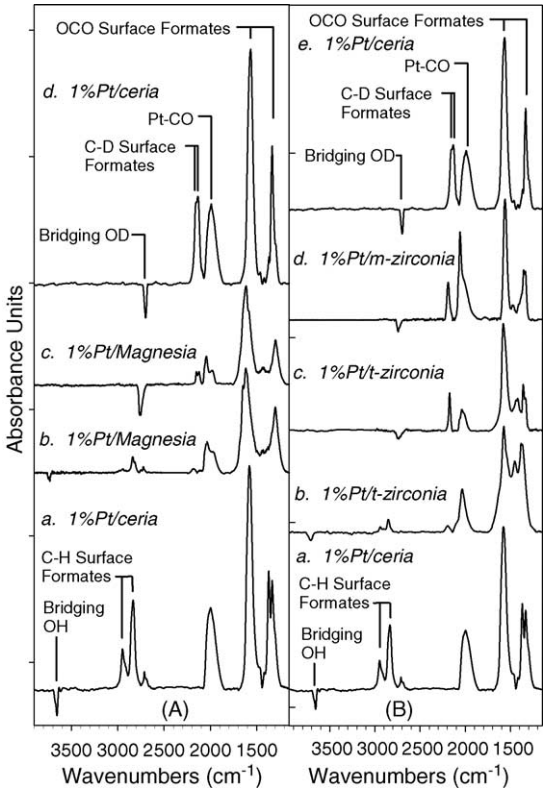

Fig. 5. (A) Comparison of formates generated from adsorption of CO at 250 °C (3.75 ccm CO:135 ccm N_2) to partially reduced Pt/ceria (H_2 or D_2 reduction, 250 °C) with those of Pt/magnesia (reduction, 450 °C), moving upward: H-formates from CO + –OH on (a) 1% Pt/ceria and (b) 1% Pt/magnesia; D-formates from CO + –OD on (c) 1% Pt/magnesia and (d) 1% Pt/ceria. (B) Comparison of formates generated from adsorption of CO to Pt/ceria (H_2 or D_2 reduction 250 °C) with those of Pt/zirconia, moving upward: H-formates from CO + –OH on (a) 1% Pt/ceria and (b) 1% Pt/t-zirconia. D-formates from CO + –OD on (c) 1% Pt/t-zirconia, (d) 1% Pt/m-zirconia, and (e) 1% Pt/ceria. Prior to CO adsorption, treatment with H_2:N_2 or D_2:N_2 mixture in the ratio 100 ccm:135 ccm was carried out, followed by a nitrogen purge (135 ccm).

Therefore, we carried out CO adsorption to these related materials at 250 °C, after hydrogen treatment and purging with N_2, and the results are displayed in Fig. 5A for Pt/magnesia and Fig. 5B for Pt/zirconia catalysts. Since the detector response curve in infrared spectroscopy is generally low at wavenumbers above 3500 cm^{-1}, and since there was excessive absorption particularly in the background spectra of the zirconia catalysts, in addition to experiments with H_2, we carried out the experiments with D_2.

As shown in the figures, accompanying a decrease in bridging OH (or OD) groups, there is clearly the formation of formates on the surface. In comparison with the spectra of Pt/ceria catalysts, which show the most intense formate bands of all the catalysts, the positions of the OCO asymmetric and symmetric bands of the Pt/MgO and Pt/ZrO_2 catalysts, accompanied by the C–H (or C–D) stretching bands, are in close proximity to the bands observed for Pt/ceria, identifying the species as surface formates. The positions of the formate bands are tabulated in Table 1. The positions of the formate

Table 1
Formate bands observed on Pt/zirconia (this work) and magnesia catalysts

Formate designation	C–H band position (cm^{-1})	OCO asymmetric position (cm^{-1})	OCO symmetric position (cm^{-1})
Magnesia			
α-formate[a]	2811	1649	1304
β-formate[a]	2750, 2715	1610	1388
γ-formate[a]	2839	1622	1342
Pt/Zirconia			
Formates	2860, 2950	ca. 1580	ca. 1350

[a] Notation and assignments reproduced from [23].

bands observed in this work are similar to those observed previously by Shido et al. [23], which are shown in the table. The major C–H band in this work was found to be that of the γ-formate, observed at slightly lower wavenumbers (ca. 2830 cm^{-1}) than reported in [23].

As depicted in Fig. 6, the surface formate concentrations as measured by the C–H and C–D bands were regulated by the WGS rate (for temperatures 250, 300, and 350 °C) at high H_2O/CO ratios (3.75 ccm CO:125 ccm H or D-water:10 ccm N_2), as we have previously observed in the case of Pt/ceria [6,7]. These findings are consistent with the response of a reaction intermediate.

Utilizing CO as a probe molecule of the bridging OH groups, the relative ranking of formate intensities after CO adsorption was found to be: Pt/ceria > Pt/m-zirconia > Pt/t-zirconia > Pt/magnesia. Furthermore, the monoclinic zirconia sample was found to have a lower selectivity for carbonate formation compared with the tetragonal sample, the OCO carbonate bands appearing in the region between 1390 and 1475 cm^{-1}. This finding may indicate differences in surface acidity resulting from the differences in the preparation procedures utilized, or from the nature of the surfaces due to slight differences in the surface atomic arrangements. From the standpoint of applied catalysis, we have suggested that the formate intensities resulting from CO adsorption may provide catalyst developers with a tool for predicting WGS activity [7], since the CO is essentially probing the active site densities of the bridging OH groups.

It is clear from the XANES experiments (Fig. 4) with Pt/zirconia and Pt/ceria, that the extent of surface reduction is quite different. We used a linear combination of XANES reference spectra in order to better quantify the degree of reduction in hydrogen treatment. While the reduction of Pt/ceria at 300 °C led to values of Ce^{4+} of 77.5% and Ce^{3+} of 22.5%, the reduction on Pt/zirconia appears to be much more limited. Considering this, the finding that the formates were lower in intensity in the case of the zirconia catalysts by infrared spectroscopy is consistent with a lower number of bridging OH groups associated with reduced centers. Since defect formation in magnesia is more energy intensive, it is not surprising that their population would be even lower than that of zirconia, resulting in the lowest formate band intensities during CO adsorption of the series.

3.5. Catalytic activity and the normal kinetic isotope effect

It is evident from Figs. 7a and 8a that catalytic activity correlates with the formate band intensities very well, with

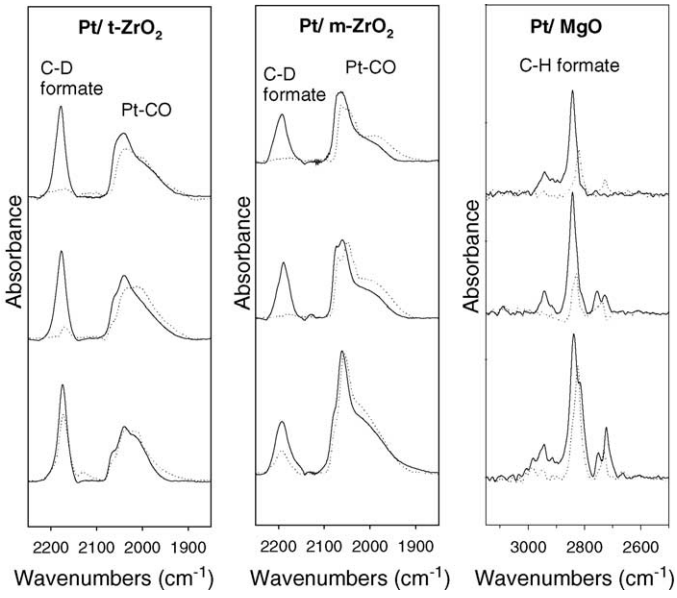

Fig. 6. DRIFTS difference spectra after adsorption of CO to Pt/t-ZrO_2, Pt/m-ZrO_2, and Pt/MgO at, moving upwards, 250, 300, and 350 °C. Pt/ZrO_2 catalysts were pretreated in 100 ccm D_2:135 ccm N_2, while Pt/MgO was pretreated in 100 ccm H_2:135 ccm N_2. Catalysts were purged in 135 ccm N_2 before adsorption of CO. Dotted line spectra show response of formates after replacing N_2 balancing gas with 125 ccm D_2O (for Pt/ZrO_2 catalyst) or H_2O (for Pt/MgO). At a high H_2O/CO or D_2O/CO ratio, while the Pt–CO band changes very little with steam addition, the surface formate coverages are controlled by the WGS rate, becoming increasingly reaction rate limited with temperature.

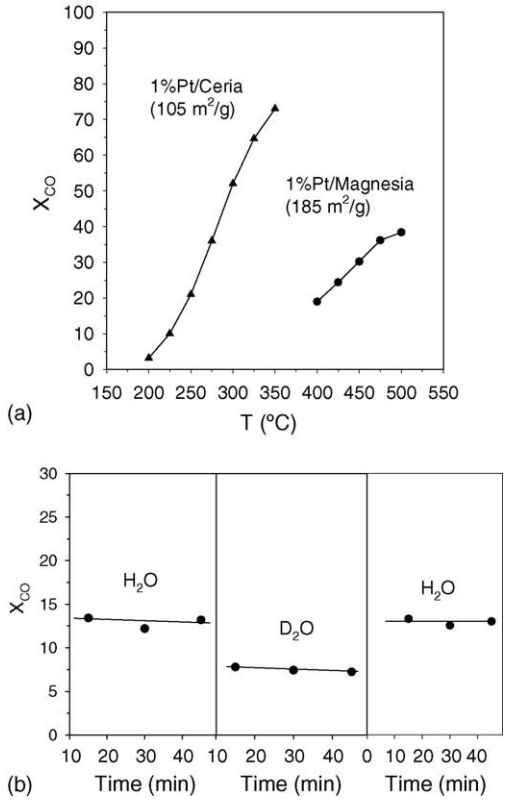

Fig. 7. (a) Comparison of the activity of 1% Pt/magnesia (185 m^2/g) to 1% Pt/ceria (105 m^2/g). Testing was conducted in a fixed bed reactor using 3.75 ccm CO:100 ccm H_2:125 H_2O:10 ccm N_2 and 33 mg catalyst. (B) Normal kinetic isotope effect observed between switching from feed containing H_2:H_2O to D_2:D_2O in the fixed bed reactor (testing at 400 °C) for Pt-MgO.

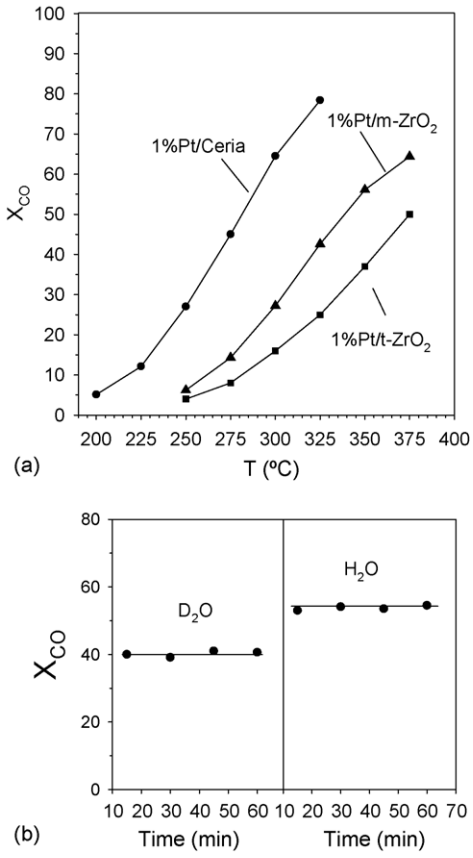

Fig. 8. (a) Comparison of the activity of 1% Pt/zirconia monoclinic and tetragonal catalysts to 1% Pt/ceria (105 m^2/g). Testing was conducted in a fixed bed reactor using 3.75 ccm CO:100 ccm H_2:125 H_2O:10 ccm N_2 and 33 mg catalyst. (b) Normal kinetic isotope effect observed at 300 °C using feed containing 3.75 ccm CO:125 ccm D_2O (or H_2O) for Pt-t-ZrO_2.

the activity of Pt/ceria > Pt/m-zirconia > Pt/t-zirconia > Pt/magnesia. Therefore, there appears to be an important link between the number of bridging OH groups (i.e., active sites), as probed by CO adsorption, and the resulting catalytic activity. Since the bridging OH groups are associated with defect centers (i.e., vacancies), the ability of the oxide to change oxidation state at the surface (or form a defect) is one important characteristic when considering the selection of an oxide component for WGS.

As noted in Section 1, it has been found that on most metals and oxides, formates generated from adsorption of formic acid are stable enough, so that it is the second step (i.e., decomposition of the formate) that is the rate-limiting step, and the selectivity is governed by the choice of catalyst. In the case of Pt/ceria, the formates produced from adsorption of CO are very intense in IR spectroscopy, and are quite stable in the low temperature shift range. We have found that identical formates are produced whether or not the partially reduced ceria (i.e., with bridging OH groups) reacted with formic acid or by adsorption of CO. However, formates rapidly decompose in the presence of H_2O [50].

Shido and Iwasawa have given numerous examples (ZnO [24], MgO [23], and Rh/ceria [14]) which have linked the normal kinetic isotope effect of WGS to the decomposition of the pseudo-stable formate by H_2O. For example, they conducted tests using a recirculating reactor, and found a normal KIE in switching between H_2O and D_2O. The same KIE was observed in the decomposition rates of the stabilized H and D-formates. However, from the infrared experiments of the decomposition of formates, the KIE depends on whether it is a C–H or a C–D in the formate but it does not depend on whether H_2O or D_2O is used to carry out the decomposition. We have recently reproduced the results of Shido and Iwasawa with experiments of noble metal promoted ceria [49,50]. The normal KIE involved in decomposing the stabilized formate with H_2O is approximately 1.4, and the same value of 1.4 is obtained from reactor testing.

Finally, it is important to correlate the DRIFTS findings with the decomposition of formic acid studies. We have recently observed identical surface formates on Pt/ceria by adsorption of formic acid as was produced from the reaction of CO with the bridging OH groups. In a fixed bed reactor, we switched between HCOOH and DCOOH to carry out the formic acid decomposition and obtained a similar KIE of 1.3 [27]. The results strongly suggest that C–H bond cleaving is linked to the rate-imiting step of both formic acid decomposition and WGS.

Figs. 7b and 8b display the normal kinetic isotope effect in switching between H_2O and D_2O for Pt/magnesia and Pt/zirconia, respectively. The KIE was about 1.55 for Pt/magnesia, very close to the results reported by Shido et al. [23] and approximately 1.3 for Pt/zirconia, indicating that a mechanism involving formate intermediates is likely. C–H bond cleaving during the rate-limiting step is also predicted based on a theoretical model of formic acid decomposition occurring on MgO surfaces with defects [47].

4. Conclusions

During reduction in hydrogen, Pt was found to catalyze the decomposition of surface carbonates from the surface of both magnesia and zirconia, thereby facilitating the generation of active OH groups on the oxide surface. Comparison of the OH groups after surface reduction of Pt/zirconia and Pt/magnesia with those found on Pt/ceria suggested that the OH groups involved in generation of formates upon adsorption of CO are likely those of the bridging variety (i.e., type II) occurring at defect sites. The lower extent of vacancy formation for zirconia, and especially, magnesia, catalysts loaded with Pt in comparison with Pt/ceria likely explains the lower intensity of active bridging OH groups observed. A much lower surface concentration of formates was observed when CO was utilized as a probe molecule of the bridging OH groups for both Pt/magnesia and Pt/zirconia catalysts than for Pt/ceria. In comparison to Pt/ceria, the Pt/zirconia and Pt/magnesia catalysts exhibited considerably lower CO conversion during WGS. The trends in formate intensity with CO adsorption, as well as WGS activity were in the order Pt/ceria > Pt/m-zirconia > Pt/t-zirconia > Pt/magnesia. In all cases, a normal kinetic isotope effect was found in switching from H_2O to D_2O, in agreements with a link between the rate-limiting step and the decomposition of surface formates, which was previously put forth by Shido and Iwasawa.

Acknowledgement

This work was supported by the Commonwealth of Kentucky.

References

[1] Fuel Cell Handbook, 5th ed., US DOE, NETL, 2000.
[2] Fuel Cells for Transportation Program Contractors' Annual Progress Report, US DOE, OAAT, 1998.
[3] D.C. Dayton, M. Ratcliff, R. Bain, Fuel cell integration—a study of the impact of gas quality and impurities, NREL/MP-510-30298, 2001.
[4] A.F. Ghenciu, Curr. Opin. Solid State Mater. Sci. 6 (2002) 389–399.
[5] R. Farrauto, S. Hwang, L. Shore, W. Ruettinger, J. Lampert, T. Giroux, Y. Liu, O. Ilinich, Annu. Rev. Mater. Res. 33 (2003) 1.
[6] G. Jacobs, L. Williams, U. Graham, D. Sparks, B.H. Davis, J. Phys. Chem. B 107(38) 10398.
[7] G. Jacobs, L. Williams, U. Graham, D. Sparks, G. Thomas, B.H. Davis, Appl. Catal. A 252 (2003) 107.
[8] G. Jacobs, P.M. Patterson, L. Williams, E. Chenu, D. Sparks, G. Thomas, B.H. Davis, Appl. Catal. A 262 (2004) 177.
[9] T. Bunluesin, R. Gorte, G. Graham, Appl. Catal. B 15 (1998) 107.
[10] S. Hilaire, X. Wang, T. Luo, R.J. Gorte, J. Wagner, Appl. Catal. 215 (2001) 271.
[11] X. Wang, R.J. Gorte, Appl. Catal. A 247 (2003) 157.
[12] Y. Li, Q. Fu, M. Flytzani-Stephanopoulos, Appl. Catal. B 27 (2000) 179.
[13] Q. Fu, A. Weber, M. Flytzani-Stephanopoulos, Catal. Lett. 77 (1–3) (2001) 87.
[14] T. Shido, Y. Iwasawa, J. Catal. 141 (1993) 71.
[15] T. Shido, Y. Iwasawa, J. Catal. 136 (1992) 493.
[16] P. Mars, in: J.H. de Boer, et al. (Eds.), Proceedings of the Symposium on the Mechanism of Heterogeneous Catalysis, Elsevier, Amsterdam, The Netherlands, 1959.
[17] P. Mars, J.J.F. Scholten, P. Zwietering, Adv. Catal. 14 (1963) 35.
[18] K. Tamaru, Trans. Faraday Soc. 55 (1959) 824.
[19] K. Tamaru, Bulletin of the Faculty of Engineering, vol. 8, Yokohama National University, 1959 p. 81.
[20] J. Fahrenfort, L. van Reijen, W.M.H. Sachtler, in: Proceedings of the Symposium on the Mechanism of Heterogeneous Catalysis, Elsevier, Amsterdam, The Netherlands, 1960.
[21] K. Hirota, K. Kuwata, Y. Nakai, Bull. Chem. Soc. Jpn. 31 (1958) 861.
[22] C. Li, K. Domen, K. Maruya, T. Onishi, J. Catal. 125 (1990) 445.
[23] T. Shido, K. Asakura, Y. Iwasawa, J. Catal. 122 (1990) 55.
[24] T. Shido, Y. Iwasawa, J. Catal. 129 (1991) 343.
[25] T. Shido, Y. Iwasawa, J. Catal. 136 (1992) 493.
[26] C. Li, Y. Sakata, T. Arai, K. Domen, K. Maruya, T. Onishi, J. Chem. Soc., Faraday Trans. 85 (1989) 1451.
[27] G. Jacobs, P.M. Patterson, U.M. Graham, A.C. Crawford, B.H. Davis, submitted for publication.
[28] A. Holmgren, B. Andersson, D. Duprez, Appl. Catal. B 22 (1999) 215.
[29] A. Laachir, V. Perrichon, A. Badri, J. Lamotte, E. Catherine, J.C. Lavalley, J. El Fallah, L. Hilaire, F. Le Normand, E. Quemere, G.N. Sauvion, O. Touret, J. Chem. Soc., Faraday Trans. 87 (1991) 1601.
[30] C. Binet, A. Badri, J.C. Lavalley, J. Phys. Chem. 98 (1994) 6392.
[31] S. Overbury, D. Huntley, D. Mullins, G. Glavee, Catal. Lett. 51 (1998) 133.
[32] J. El Fallah, S. Boujani, H. Dexpert, A. Kiennemann, J. Majerus, O. Touret, F. Villain, F. Le Normand, J. Phys. Chem. 98 (1994) 5522.
[33] J. Lamotte, J.C. Lavalley, E. Druet, E. Freund, J. Chem. Soc., Faraday Trans. 79 (1983) 2219.
[34] G. Jacobs, A.C. Crawford, L. Williams, P.M. Patterson, B.H. Davis, Appl. Catal. A 267 (2004) 27.
[35] K. Jung, A.T. Bell, J. Catal. 193 (2000) 207.
[36] J. Kondo, Y. Sakata, K. Domen, K. Maruya, T. Onishi, J. Chem. Soc., Faraday Trans. 86 (1990) 397.
[37] M.W. Balakos, M.R. Madden, T.L. Walsh, J.P. Wagner, in: Proceedings of the AICHE Spring National Meeting, New Orleans, LA, USA, April, 2004.
[38] D. Eder, R. Kramer, PCCP 4 (2002) 795.
[39] S.M. Stagg-Williams, F.B. Noronha, G. Fendley, D.E. Resasco, J. Catal. 194 (2000) 240.
[40] R. Srinivasan, O.B. Cavin, C.R. Hubbard, B.H. Davis, J. Am. Ceram. Soc. 75 (1992) 1217.
[41] R. Srinivasan, O.B. Cavin, C.R. Hubbard, B.H. Davis, Chem. Mater. 5 (1993) 27.
[42] D.A. Skoog, D.M. West, F.J. Holler, Fundamentals of Analytical Chemistry, 6th ed. Saunders College Publishing, Fort Worth, TX, 1992.
[43] A. Clearfield, Inorg. Chem. 3 (1964) 146.
[44] R. Srinivasan, R.J. de Angelis, G. Ice, B.H. Davis, J. Mater. Res. 6 (1991) 1287.

[45] A.L. Almeida, J.B.L. Martins, E. Longo, C.A. Taft, J. Murgich, A.F. Jalbout, J. Mol. Struct. (Theochem.) 664/665 (2003) 111.
[46] M. Lintuluoto, H. Nakatsuji, M. Hada, H. Kanai, Surf. Sci. 429 (1999) 133.
[47] S.M. Stagg-Williams, D.E. Resasco, Stud. Surf. Sci. Catal. 130 (2000) 3663.
[48] F.B. Noronha, C. Taylor, E.C. Fendley, S.M. Stagg-Williams, D.E. Resasco, Catal. Lett. 90 (2003) 13.
[49] G. Jacobs, S. Khalid, P.M. Patterson, D.E. Sparks, B.H. Davis, Appl. Catal. 268 (2004) 255.
[50] G. Jacobs, P.M. Patterson, U. Graham, D. Sparks, B.H. Davis, Appl. Catal. 269 (2004) 63.